PENSOFT

SENCKENBERG
world of biodiversity

Leibniz Association

Comparative analysis of complete mitochondrial genomes of Panorpidae (Insecta: Mecoptera) and new perspectives on the phylogenetic position of *Furcatopanorpa*

Yuan Hua[1,2], Ning Li[3], Jian Su[1], Baozhen Hua[3], Shiheng Tao[2], Lianxi Xing[1]

1 *College of Life Sciences, Northwest University, Xi'an, Shaanxi 710069, China*

2 *College of Life Sciences, Northwest A&F University, Yangling, Shaanxi 712100, China*

3 *College of Plant Protection, Northwest A&F University, Yangling, Shaanxi 712100, China*

https://zoobank.org/A0FC7F1B-5838-4DEB-92F4-1A0F2FE7F1FE

Corresponding authosr: Shiheng Tao (shihengt@nwafu.edu.cn), Lianxi Xing (lxxing@nwu.edu.cn)

Received 27 April 2023
Accepted 6 December 2023
Published 18 March 2024

Academic Editors Christiane Weirauch, Marianna Simões

Citation: Hua Y, Li N, Su J, Hua B, Tao S, Xing L (2024) Comparative analysis of complete mitochondrial genomes of Panorpidae (Insecta: Mecoptera) and new perspectives on the phylogenetic position of *Furcatopanorpa*. Arthropod Systematics & Phylogeny 82: 119–131. https://doi.org/10.3897/asp.82.e105560

Abstract

The scorpionfly genus *Furcatopanorpa* Ma & Hua, 2011 is a monotypic taxon of Panorpidae with a series of unique characters. However, the phylogenetic position of *Furcatopanorpa* in Panorpidae has not been satisfactorily resolved yet. Based on 48 complete mitochondrial genomes, we analyzed the mitochondrial phylogenomics and phylogeny of representatives of Panorpidae. The phylogenetic analyses indicate that *Furcatopanorpa* and *Neopanorpa* form a sister group relationship with high support. The chronogram of Panorpidae shows that *Furcatopanorpa* and *Neopanorpa* separated at ca. 82.07 Ma, while the species of *Neopanorpa* shared the most recent common ancestor at 49.07 Ma. Judged from the topology of the phylogenetic trees, it seems unsuitable to assign *Furcatopanorpa* into the subfamily Panorpinae, because this assignment may cause Panorpinae to be a paraphyletic group. A putative conclusion might be that *Furcatopanorpa* may need to be raised to subfamily status.

Keywords

Mecoptera; Mitogenome; Panorpidae; Phylogeny; Scorpionflies

1. Introduction

The scorpionfly genus *Furcatopanorpa* Ma & Hua, 2011 is a monotypic taxon of Panorpidae (Insecta: Mecoptera), with *Panorpa longihypovalva* Hua & Cai, 2009 as its type species. The genus is distinguishable from other confamilial genera by a suite of unique characters, especially the absence of notal organ on male tergum 3, and atypical O-shaped mating pattern (Hua and Cai 2009; Ma and Hua 2011; Zhong et al. 2015). The seventh and eighth abdominal segments of males are shortened and not constricted basally; and the hypovalvae of male genitalia are extremely elongated and parameres are extraordinarily developed with complicated lobes. The peculiar feature

of the male reproductive system lies in the position of the epididymis, which is separated from the base of the testis within a peritoneal sheath, not pressed against the lateral base of the testis as in other genera of Panorpidae (Zhang et al. 2016). The ejaculatory ducts comprise a median duct and an accessory sac (Lyu et al. 2022). The axis of female medigynium is forked distally.

The genus *Furcatopanorpa* has a peculiar mating pattern. The male maintains copulation by continuous provision of salivary secretion to the female (Zhong et al. 2015), instead of by seizing the female with grasping devices as in other Panorpidae (Thornhill 1981). During copulation, the well-developed multi-branched male salivary glands continually provide liquid secretion through a mouth-to-mouth mode to the female (Zhong et al. 2015). Cytogenetically, *Furcatopanorpa* is characterized by large heterochromatic blocks, a chromosome number of n = 21, with the sex determination mechanism as XX/XO type (Miao et al. 2019).

Based on phylogenetic analyses from molecular and morphological data (Hu et al. 2015; Miao et al. 2019, Wang and Hua 2021), the Panorpidae are grouped into two subfamilies. The subfamily Neopanorpinae consists of *Neopanorpa* van der Weele, 1909, *Leptopanorpa* McLachlan, 1875, and two newly erected genera *Lulilan* Willmann, 2022 and *Phine* Willmann, 2022 (Willmann 2022), while the subfamily Panorpinae comprises all the other genera. However, the phylogenetic position of *Furcatopanorpa* remains controversial. *Furcatopanorpa* was considered a sister taxon to all other genera of Panorpidae by Ma et al. (2012), but was regarded to form a sister taxon to some species of *Panorpa* (Hu et al. 2015; Miao et al. 2019; Wang and Hua, 2021).

The mitochondrial genome (or mitogenome) of insects is a double-stranded circular molecule, varying in length from 14 to 20 kb (Cameron 2014). The mitogenome is characterized by simple genetic structure, small size, maternal inheritance, high copy numbers, less recombination, and fast evolutionary rate (Boore 1999), thus being regarded as a valuable tool for population genetics, species delimitation, and phylogenetic analyses in numerous groups of insects (Dowton et al. 2002; Wang et al. 2013, 2019; Choudhary et al. 2015; Song et al. 2016). Mitochondrial genomes may provide further evidence for the phylogenetic analysis of Panorpidae.

In this study, we sequenced 43 mitochondrial genomes of Panorpidae in order to decipher the phylogenetic position of *Furcatopanorpa* in Panorpidae.

2. Materials and methods

2.1. Taxon sampling and DNA extraction

Adults were captured from various mountain regions in China from 2019 to 2021 (Table 1). All specimens were preserved in 100% ethanol at −20°C and identified to species through morphological characters (Wang and Hua 2018). Total genomic DNA was extracted individually from one-side legs using DNeasy DNA Extraction Kit (Qiagen) according to the manufacturer's protocol. Voucher specimens are kept at the Entomological Museum, Northwest A&F University.

2.2. Sequence analyses

The whole mitochondrial genome sequences were generated using Illumina HiSeq™2500 with paired reads of 2 × 150 bp by the Biomarker Technologies Co., LTD (Beijing, China). The raw data was subjected to fastp quality control filtering to obtain Clean Data (Chen et al. 2018). Assembly and annotation were conducted using MitoZ v2.3 (Meng et al. 2019) and then checked by manual proofreading according to its relative species from NCBI. All the 13 PCGs (protein coding genes) were determined by the ORF Finder employing codon table 5 and compared with the homologous sequence of the reference mitogenome. Two rRNA genes were predicted by comparing with the homologous sequence of other Panorpidae mitogenomes and the locations of adjacent genes. Twenty-two tRNA genes were identified using the MITOS Web Server (http://mitos.bioinf.uni-leipzig.de/index.py) employing codon table 5 (Bernt et al. 2013). The control region was determined by the locations of adjacent genes. Tandem repeat units of the control regions were identified by the Tandem Repeats Finder server (http://tandem.bu.edu/trf/trf.html) (Benson 1999). Mitogenomic circular maps were generated using Organellar Genome DRAW (https://chlorobox.mpimp-golm.mpg.de/OGDraw.html) (Lohse et al. 2013).

Analyses of the sequenced mitogenomes were calculated using PhyloSuite 1.2.2 (Zhang et al. 2020), including the base composition, mitogenomic organization tables, and relative synonymous codon usage (RSCU) values. The sliding window analysis (a sliding window of 200 bp and step size of 25 bp), the nucleotide diversity (π) of 13 PCGs and two rRNAs among 48 mitogenomes of Panorpidae were conducted using DnaSP 6.0 (Rozas et al. 2003). We analyzed the genetic distances based on Kimura-2-parameter and the ratios between non-synonymous (Ka) and synonymous substitutions rates (Ks) of 13 PCGs among the 48 mitogenomes using MEGA X (Kumar et al. 2018) and DnaSP 6.0 (Rozas et al. 2003), respectively. AT- and GC-skews were used to measure the strand bias of the nucleotide composition of mitogenomes (Hassanin 2006).

2.3. Phylogenetic analyses

A total of 50 mitogenomes were used in the phylogenetic analyses, including 48 mitogenomes of Panorpidae as the ingroup and two mitogenomes of Panorpodidae as the outgroup (Table 1). The extractions of 13 PCGs, 22 tRNAs, and two rRNAs were conducted with PhyloSuite 1.2.2 (Zhang et al. 2020). The nucleotide sequences

Table 1. Information of the species and mitogenomes used in this study.

Species	Locality	Size (bp)	Accession no.
Cerapanorpa brevicornis	Huoshaodian, Shaanxi	16337	OR941459
Cerapanorpa byersi	Tongtianhe Forest Park, Shaanxi	16317	OR941460
Cerapanorpa dubia	Zhuque Forest Park, Shaanxi	16322	OR941461
Cerapanorpa nanwutaina TTH	Tongtianhe Forest Park, Shaanxi	16312	OR941462
Cerapanorpa nanwutaina ZQ	Zhuque Forest Park, Shaanxi	16328	OR941463
Cerapanorpa obtusa	—	16318	KX091860
Dicerapanorpa magna LP	Liping Forest Park, Shaanxi	16449	OR941464
Dicerapanorpa magna MCS	Micangshan, Sichuan	16452	OR941465
Dicerapanorpa magna TTH	Tongtianhe Forest Park, Shaanxi	16455	OR941466
Dicerapanorpa magna WLD	Wulongdong, Shaanxi	16452	OR941467
Dicerapanorpa minshana 1	Tangjiahe, Sichuan	16444	OR941468
Dicerapanorpa minshana 2	Tangjiahe, Sichuan	16449	OR941469
Dicerapanorpa minshana 3	Tangjiahe, Sichuan	16446	OR941470
Furcatopanorpa longihypovalva HSD	Huoshaodian, Shaanxi	17123	OR941471
Furcatopanorpa longihypovalva LP	Liping Forest Park, Shaanxi	17088	OR941472
Furcatopanorpa longihypovalva MCS	Micangshan, Sichuan	17080	OR941473
Furcatopanorpa longihypovalva TTH	Tongtianhe Forest Park, Shaanxi	17051	OR941474
Neopanorpa brisi	Yangjiahe, Yunnan	16339	OR941475
Neopanorpa chelata	Linggongli, Sichuan	16337	OR941476
Neopanorpa chelata	—	16342	KX091857
Neopanorpa claripennis 1	Tangjiahe, Sichuan	16358	OR941477
Neopanorpa claripennis 2	Tangjiahe, Sichuan	16359	OR941478
Neopanorpa claripennis 3	Tangjiahe, Sichuan	16369	OR941479
Neopanorpa longiprocessa 1	Huoditang, Shaanxi	16337	OR941480
Neopanorpa longiprocessa 2	Huoditang, Shaanxi	16328	OR941481
Neopanorpa lui	Wulongdong, Shaanxi	16367	OR941482
Neopanorpa nielseni	Daxueshan, Yunnan	16222	OR941483
Neopanorpa pulchra	Jianfengling, Hainan	16314	JX569848
Neopanorpa pulchra	—	15531	FJ169955
Neopanorpa quadristigma	Tanglishan, Yunnan	16272	OR941484
Neopanorpa triangulata	Tanglishan, Yunnan	16307	OR941485
Panorpa chengi	Lipingcun, Shaanxi	16426	OR941486
Panorpa curva	Wolong Nature Reserve, Sichuan	16375	OR941487
Panorpa debilis	Cliffs Forest of rare Charitable Research Reserve, Cambridge	17018	MK870081
Panorpa dispergens	Baishuitai, Yunnan	16383	OR941488
Panorpa fulvastra 1	Jiuhuangshan, Sichuan	16279	OR941489
Panorpa fulvastra 2	Jiuhuangshan, Sichuan	16278	OR941490
Panorpa fulvastra 3	Jiuhuangshan, Sichuan	16277	OR941491
Panorpa fulvastra HDT	Huoditang, Shaanxi	16345	OR941492
Panorpa sp1	Xiaozhaizigou, Sichuan	16304	OR941493
Panorpa sp2	Xiaozhaizigou, Sichuan	16289	OR941494
Panorpa sp3	Xiaozhaizigou, Sichuan	16328	OR941495
Panorpodes kuandianensis 1	Huaboshan, Liaoning	16425	unpublished
Panorpodes kuandianensis 2	Huaboshan, Liaoning	16427	unpublished
Sinopanorpa digitiformis 1	Hualongshan, Shaanxi	16394	OR941496
Sinopanorpa digitiformis 2	Hualongshan, Shaanxi	16399	OR941497
Sinopanorpa nangongshana 1	Nangongshan, Shaanxi	16378	OR941498
Sinopanorpa nangongshana 2	Nangongshan, Shaanxi	16479	OR941499
Sinopanorpa nangongshana 3	Nangongshan, Shaanxi	16358	OR941500
Sinopanorpa tincta	Tongtianhe Forest Park, Shaanxi	16386	OR941501
Note: The capital letter markers indicate the collection locations; the numeric marks indicate different samples from the same location.			

were aligned in batches with MAFFT (Katoh and Standley 2013) integrated into PhyloSuite 1.2.2 and the ambiguous sites were removed using Gblocks (Talavera and Castresana 2007). The concatenations of genes were conducted using PhyloSuite 1.2.2.

Phylogenetic trees were reconstructed for six genera of Panorpidae using Bayesian inference (BI) and maximum likelihood (ML) analyses. In order to reduce the impact of long-branch attraction and compositional heterogeneity, a dataset with third codon position removed was included, and the site-heterogeneous mixture CAT-GTR model was used in the phylogenetic analyses (Bergsten 2005; Song et al. 2016; Nie et al. 2018). Four datasets were generated: (1) PCG: 13 PCGs (11,178 bp); (2) PCG + R: 13 PCGs and 2 rRNAs (13,380 bp); (3) PCG + R + T: 13 PCGs, 2 rRNAs, and 22 tRNAs (14,906 bp); and (4) PCG12 + R: 13 PCGs excluding third codon position + 2 rRNAs (9,654 bp). The nucleotide substitution models and partitioning strategies for Bayesian inference were chosen by PartitionFinder 2 (Lanfear et al. 2017) (Table S2). The Bayesian inference was conducted using MrBayes 3.2.6 (Ronquist et al. 2012) and performed two Markov chain Monte Carlo (MCMC) runs of 200 million generations with sampling every 100 generations. The first 25% were discarded as burn-in, and the remaining trees were used to generate the majority consensus tree and to estimate the posterior probabilities (PP). The substitution models for ML analyses were chosen using ModelFinder (Kalyaanamoorthy et al. 2017) (Table S3). ML analyses were performed by IQ-TREE integrated into PhyloSuite 1.2.2 with Ultrafast bootstrap (Nguyen et al. 2015; Zhang et al. 2020). Bootstrap support (BS) values were calculated with 1000 replicates. Bayesian analyses with a site-heterogeneous model were performed using PhyloBayes-MPI 1.9 base on the CAT-GTR model (Lartillot et al. 2013). Two independent MCMC chains would continue to run until satisfactory convergence was reached (maxdiff < 0.1). The initial 25% trees of each run were discarded as burn-in, then the consensus tree was constructed from the remaining trees combined from two runs.

2.4. Divergence time estimation

Divergence time estimates were performed based on the dataset PCG + R in BEAST 1.10.4 (Drummond et al. 2012). The substitution models of each locus for BEAST analyses were calculated in ModelFinder. The BEAST analysis was based on a Yule speciation process. Fossil evidence was used to calibrate the Bayesian estimates of divergence times (Parham et al. 2012). Based on the Ypresian fossil specimen, the fossil-calibrated node of panorpoids can be constrained to a normal distribution of 52.90 ± 0.83 Ma (Archibald et al. 2010, 2013). Two MCMC runs were conducted with a chain length of 100 million generations, sampling every 1000 generations. The sampling of posterior distribution adequate was indicated by effective sample size (ESS) > 200 in Tracer 1.7 (Rambaut et al. 2018). The first 25% of resulting trees were ignored as burn-in, and the remaining trees were combined in LogCombiner 1.8.0 (Drummond et al. 2012) and summarized as maximum clade credibility (MCC) tree using TreeAnnotator 1.8.0 (Drummond et al. 2012).

3. Results

3.1. Mitogenome organization and nucleotide composition

The newly sequenced complete mitogenomes of Panorpidae vary in length from 16,222 bp in *Neopanorpa nielseni* to 17,123 bp in *Furcatopanorpa longihypovalva* HSD (Fig. 1 and Table S1). The mitogenome consists of 13 protein-coding genes (PCGs), 2 ribosome RNA genes (rRNAs), 22 transfer RNA genes (tRNAs), and one non-coding control region (CR). Fourteen genes (4 PCGs, 2 rRNAs, and 8 tRNAs) are transcribed from the minority strand (N-strand), and the remaining 23 genes (9 PCGs and 14 tRNAs) are from the majority strand (J-strand).

The mitogenomes exhibit a strong AT nucleotide bias, ranging from 76.0% in *C. dubia*, *C. nanwutaina* TTH, and *N. chelata* to 78.2% in *N. quadristigma* (Table S1). The content of A+T ranged from 74.1% to 76.9% in PCGs, from 75.0% to 76.5% in tRNAs, from 78.3% to 79.8% in rRNAs, and from 84.3% to 87.6% in CR, respectively. The AT-skew ranged from −0.017 to 0.019, and the GC-skew from −0.183 to −0.128 (Table S1).

3.2. Protein-coding genes and codon usage

Four PCGs (*nad1*, *nad4*, *nad4L*, and *nad5*) are encoded on the minority strand (N-strand), and the remaining nine PCGs on the majority strand (J-strand) in all the mitogenomes sequenced (Fig. 1). The mitogenomes have a variety of start codon usages. Besides the canonical start codons ATN (ATA, ATT, ATG, and ATC), TTG start codon is also used. The most frequently used start codon is ATG, which is utilized in seven PCGs across all species. The non-canonical start codons TTG and TCG for *cox1* and *nad1* were found in part of the newly sequenced mitogenomes. These two kinds of unusual initiation codons also exist in *C. obtusa*. In addition to the complete stop codons TAA and TAG, partial stop codons (T or TA) are also a common feature in all panorpids studied. TAA occurs more frequently than TAG. TA is usually present as the stop codon for *cox3*, *nad4*, and *nad5*, and T− is usually used as the stop codon for *cox2*.

The amino acid compositions of PCGs and the relative synonymous codon usage (RSCU) are summarized in Figs S1 and S2. The RSCU in all Panorpidae mitogenomes is generally similar to each other. The three most frequently used amino acids — UUA (Leu2), AUU (Ile), and UUU (Phe) — are composed exclusively of U or U and A. The frequency of A and U in the third position was

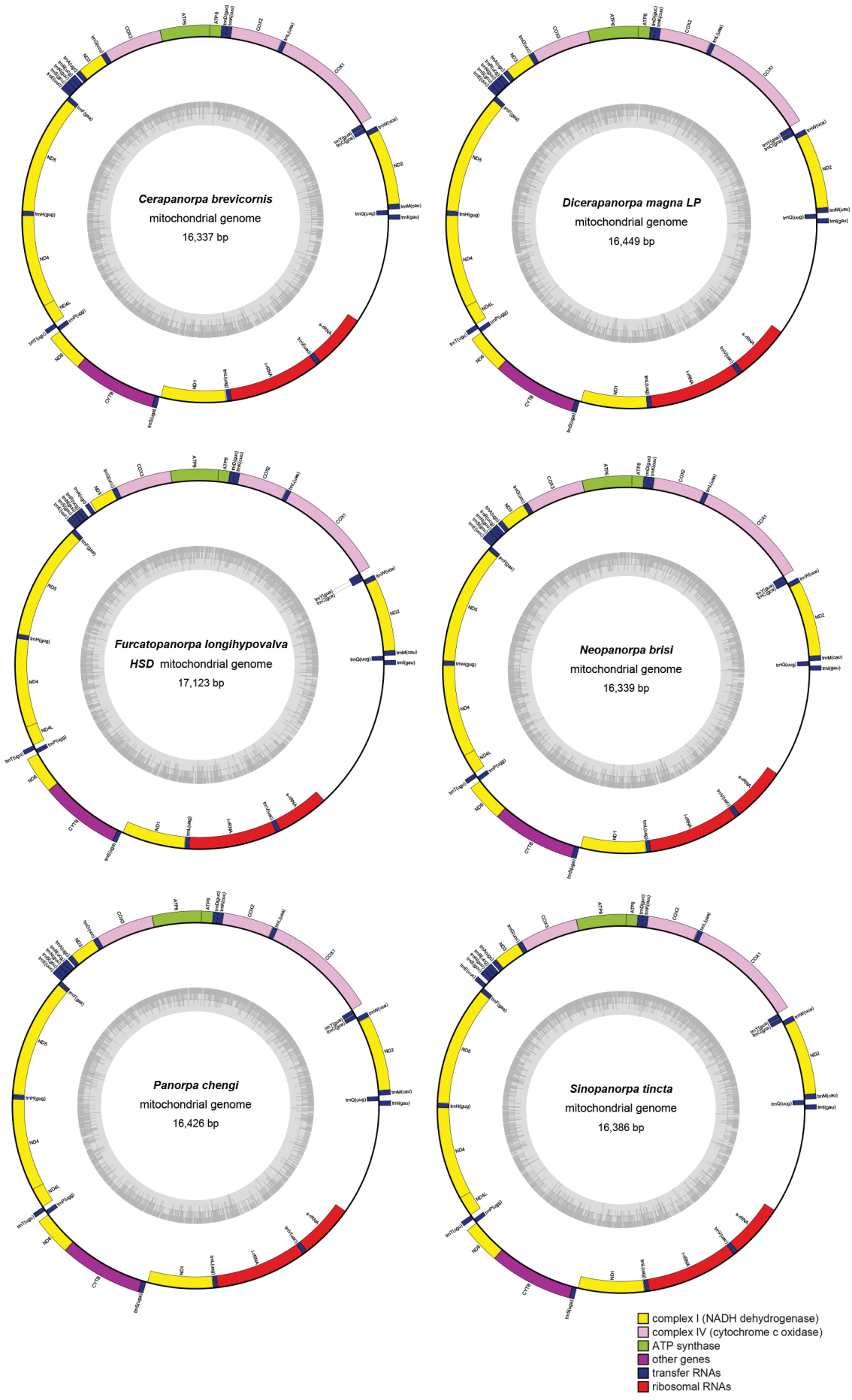

Figure 1. Circular maps of mitogenomes from representative species of Panorpidae. The J-strand is visualized on the outer circle and the N-strand on the inner circle.

much higher than C and G, reflecting AT nucleotide bias in the mitochondrial PCGs among the Panorpidae.

3.3. Transfer and ribosomal RNA genes

The mitogenomes of Panorpidae have 22 tRNA genes, which are scattered discontinuously over the entire mitogenome with eight transcribed from the N-strand and 14 from the J-strand (Fig. 1 and Table S1). The total length of 22 tRNAs ranges from 1458 to 1484 bp.

Two rRNA genes (*rrnL* and *rrnS*) are encoded on the N-strand in the mitogenomes of Panorpidae. The gene *rrnS* is located between *trnV* and the control region, and the gene *rrnL* is situated between *trnL1* and *trnV*. The average A+T content of *rrnL* (79.9%) is slightly higher than that of *rrnS* (77.1%).

3.4. Control region

The control region is the largest non-coding region located between *rrnS* and *trnI* in the mitochondrial genomes. The size of the control region ranges from 1,434 bp in *N. nielseni* to 2,252 bp in *F. longihypovalva* HSD (Fig. 2 and Table S1). The control region has the highest A+T content (84.3%−87.6%) compared with other three regions (PCGs, tRNAs, and rRNAs).

The poly-adenine (A) and $[TA(A)]_n$-like stretches were found in the control region of Mecoptera for the first time. The poly-A is randomly scattered in the control region. Most mitogenomes sequenced of the Panorpidae have tandem repeat units except for some species of *Cerapanorpa*, *Dicerapanorpa* and *Panorpa* (Fig. 2). The analyses of the control regions indicate that the length and copy number of tandem repeat units are dramatically divergent among panorpids (Fig. 2). Congeneric species may have similar tandem repeat units, e. g. *S. digitiformis* and *S. nangongshana*.

3.5. Comparative analyses of nucleotide diversity and evolutionary rate

A total of 48 mitogenomes were used in comparative analyses, including 43 newly sequenced mitogenomes together with five mitogenomes of Panorpidae downloaded from NCBI (Table 1). A sliding window analysis reveals a highly variable nucleotide diversity among the 13 PCGs and two rRNAs of the sequenced mitogenomes (Fig. S3). The values of nucleotide diversity (π values) for individual genes vary from 0.072 (*rrnL*) to 0.178 (*nad2*). The gene *nad2* exhibits the highest variability of nucleotide diversity, followed by *nad6* ($\pi = 0.176$), *nad3* ($\pi = 0.140$), and *atp8* ($\pi = 0.135$) in 13 PCGs, while *cox1* ($\pi = 0.103$), *nad1* ($\pi = 0.108$), and *atp6* ($\pi = 0.109$) exhibit comparatively low values of nucleotide diversity. The two rRNA genes show a relatively low nucleotide diversity (π = 0.072 for *rrnL* and 0.093 for *rrnS*), thus being regarded as conserved genes. The average values of pairwise genetic distances demonstrate congruent results with high genetic distances of 0.311, 0.217, and 0.170 for *nad6*, *nad2*, and *atp8*, respectively, and low genetic distances of 0.116, 0.122, and 0.125 for *cox1*, *cox2*, and *nad1*, respectively. The pairwise non-synonymous/synonymous (Ka/Ks) analyses indicate that the average Ka/Ks ratios (ω) of 13 PCGs vary from 0.027 to 0.345 (Fig. S4), suggesting that all 13 genes are under the purifying selection. The genes *atp8*, *nad6*, and *nad2* exhibit relatively high Ka/Ks ratios of 0.345, 0.305, and 0.188, respectively, whereas *cox1*, *atp6*, and *cytb* show relatively low values of 0.027, 0.049, and 0.063, respectively.

3.6. Phylogenetic analyses

The ML and BI analyses from four datasets (PCG, PCG + R, PCG + R + T, and PCG12 + R) generated trees with similar topology. The results show that the species of Panorpidae form a monophyletic group. The topologies of these trees are consistent at the genus level, but incongruent for the interspecific relationship of some species in *Cerapanorpa* and *Neopanorpa* (Figs 3, S5−S7). Phylogenetic analyses based on site-heterogeneous models show essentially the same results, with only the position of *Panorpa debilis* slightly different (Figs S8−S11). Most phylogenetic analyses indicate that the Panorpidae can be categorized into three main clades. Clade A comprises *Panorpa*, *Sinopanorpa*, *Dicerapanorpa*, and *Cerapanorpa*, while clade B consists of *Furcatopanorpa* only, and clade C is composed of *Neopanorpa* (Fig. 3).

In clade A, *Sinopanorpa*, *Dicerapanorpa*, and *Cerapanorpa* are all monophyletic. *Sinopanorpa* forms a sister group with *Cerapanorpa* in all trees, although the support values were relatively low in some cases. The North American *Panorpa debilis* is usually present as the sister taxon of *Sinopanorpa* + (*Cerapanorpa* + other species of *Panorpa*), reconfirming the paraphyly of *Panorpa*. *Dicerapanorpa* is a sister taxon to *Panorpa debilis* + *Panorpa* spp + (*Cerapanorpa* + *Sinopanorpa*) (Fig. 3).

Furcatopanorpa forms a sister group relationship with *Neopanorpa* in all trees with strong support (BS =100, PP = 1) (Figs 3 and S5−S11). In turn, *Neopanorpa* + *Furcatopanorpa* form a sister group to clade A (all the other genera studied of Panorpidae).

3.7. Divergence time

The chronogram shows that the estimated divergence time between Panorpidae and Panorpodidae is approximately at 115.09 Ma (Fig. 4). The Panorpidae began to diverge approximately at 95.35 Ma. *Neopanorpa* and *Furcatopanorpa* separated at ca. 82.07 Ma, while species of *Neopanorpa* shared the most recent common ancestor (TMRCA) at 49.07 Ma. *Cerapanorpa* and *Sinopanorpa* split from *Panorpa* at ca. 48.58 Ma, and diverged from each other approximately at 46.41 Ma. The whole clade

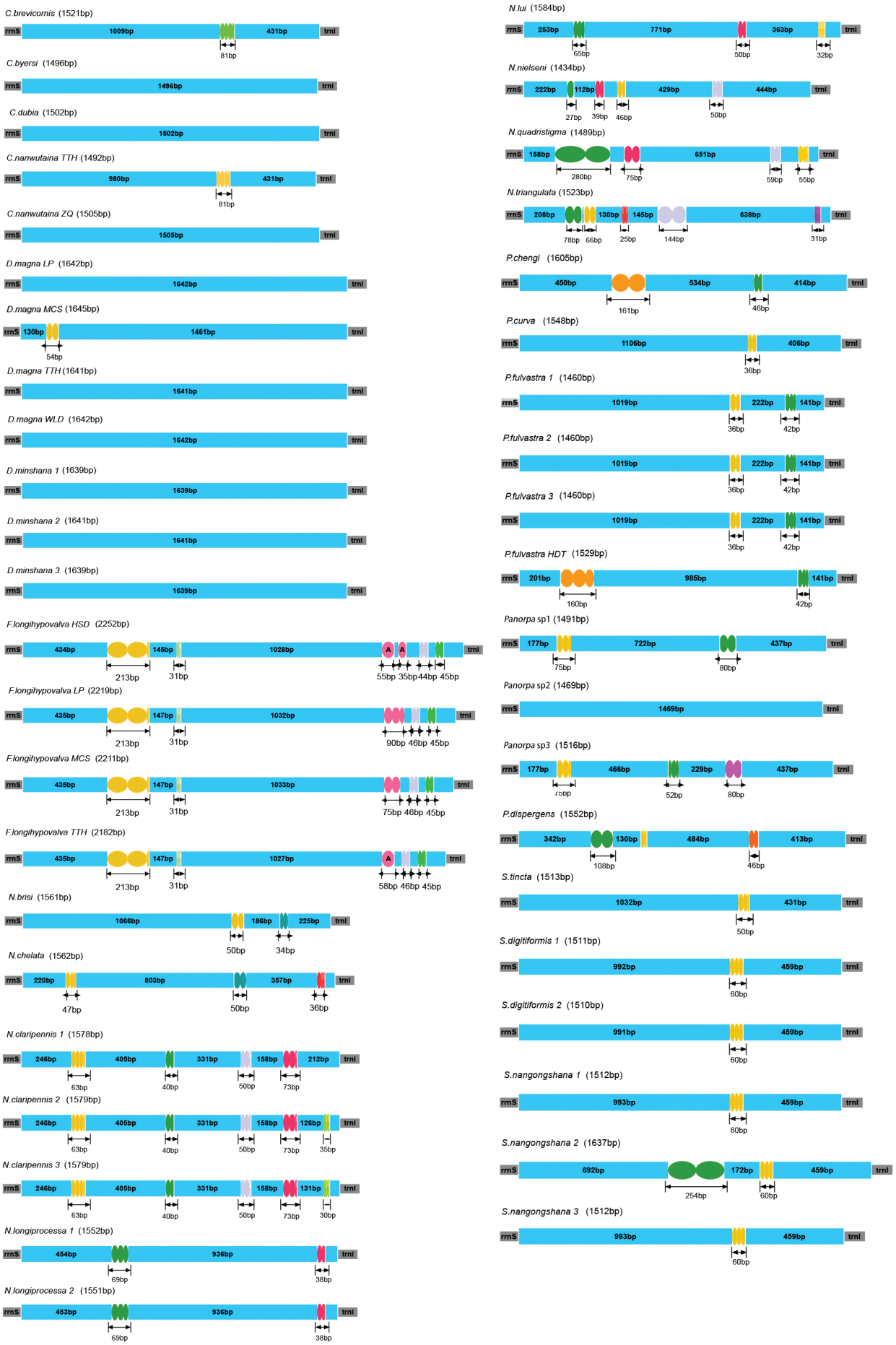

Figure 2. Organization of the control region in Panorpidae mitogenomes. The size of geometric drawings is proportional to the sequence length. The colored ovals indicate the tandem repeats; the remaining regions are shown with blue boxes.

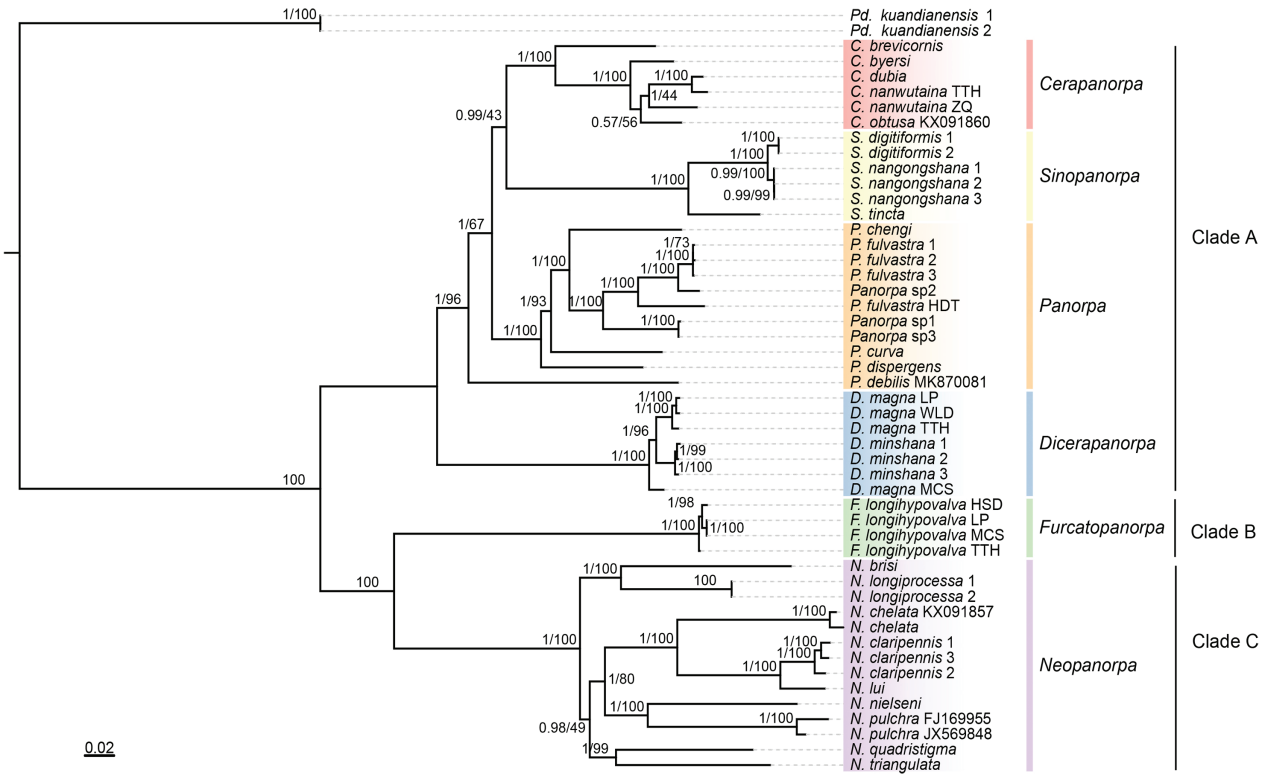

Figure 3. BI and ML trees based on the dataset of PCG + R. Numerals at nodes are the Bayesian posterior probabilities and ML bootstrap values, respectively.

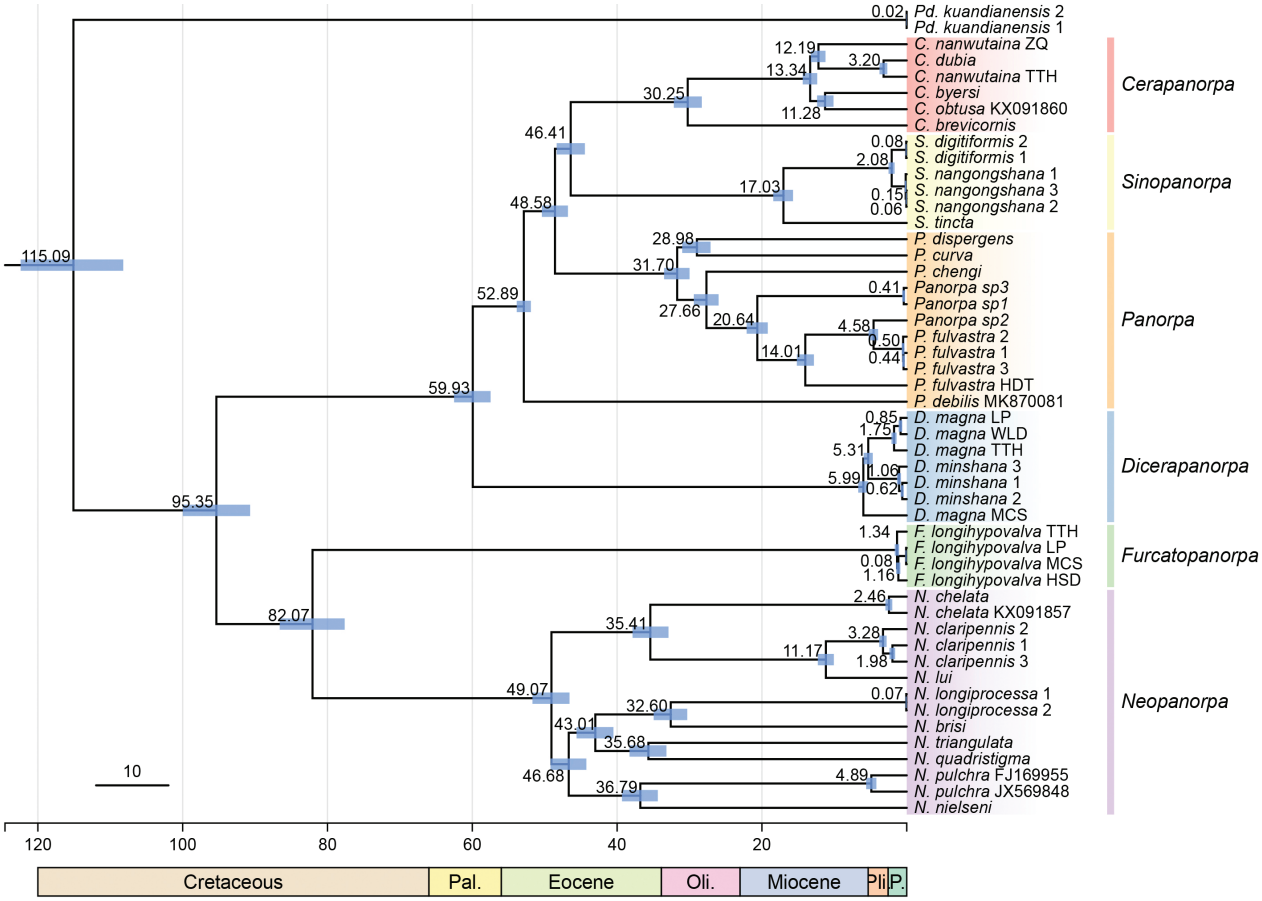

Figure 4. Chronogram of divergence time estimated from the BEAST analysis. Node numbers indicate the mean estimated divergence ages. Blue bars at nodes represent 95% highest posterior density date ranges.

including *Panorpa*, *Cerapanorpa* and *Sinopanorpa* have a common ancestor at ca. 52.89 Ma, consistent with the divergence time of the North American *Panorpa debilis* and other Eastern-Asian *Panorpa* species. The estimated divergence time between *Dicerapanorpa* and other genera in clade A is at 59.93 Ma.

4. Discussion

4.1. Mitogenome architecture

The mitogenome sequences of Panorpidae are highly conserved in the gene content, gene order, gene length, and nucleotide composition. The pattern of nucleotide skewness in whole mitogenomes is coincident with that of other mecopterans and most other insects (Wei et al. 2010). The AT-skew of whole mitogenomes of Panorpidae is slightly positive or negative, while the GC-skew is usually negative. This result is consistent with that of a recent mitochondrial genomic study in Mecoptera (Li et al. 2019).

The control region is responsible for regulating the transcription and replication of mtDNA in insects (Zhang and Hewitt 1997; Li and Liang 2018). It exhibits remarkable divergence of primary nucleotide sequences, with relatively high rates of nucleotide substitution and dramatic variation in fragment length among species or even individuals (Zhang and Hewitt 1997; Li and Liang 2018), thus being regarded as the most variable region of the mitochondrial genome. The size of the control region ranges from 1,434 to 2,252 bp in Panorpidae, but is only 898 bp in the nannochoristid *Microchorista philpotti* (Beckenbach 2011). The control region of *Furcatopanorpa* (~2,200 bp) is prominently longer than that of other confamilial genera (~1,500 to 1,600 bp). The control region structures of congeneric species are more comparable in *Cerapanorpa*, *Dicerapanorpa*, and *Sinopanorpa*. However, the structure of the control region varied considerably among individuals in *Panorpa* and *Neopanorpa*, indicating the existence of potential species groups within these two genera, consistent with a recent phylogenetic study (Wang and Hua 2021). Tandem repeat units are one of the most common structures in the control region (Li and Liang 2018). Different copy number and length of tandem repeat units are responsible for varying sizes of the control region in Panorpidae, leading to different mitogenome sizes, the so-called length heteroplasmy (Monforte et al. 1993; Zhang and Hewitt 1997; Li and Liang 2018).

Nucleotide diversity analyses are useful for identifying highly divergent nucleotide regions, which are crucial for designing species-specific markers (Jia et al. 2010; Ma et al. 2020), especially in the taxa of highly variable morphological characters. Although a fragment of 658 bp of the gene *cox1* is frequently used as a universal barcode for species delimitation in animals (Cooper et al. 2007), this gene is the least variable in the Panorpidae and has a relatively lower ratio of Ka/Ks among the PCGs in these sequenced mitogenomes. Therefore, *cox1* is difficult to afford the task of DNA barcoding in Panorpidae. Other genes with rapid evolutionary rates, alternatively, should be evaluated as potential barcode candidates (Lobry 1995; Demari-Silva et al. 2015; Zhang et al. 2018).

4.2. Phylogenetic status of *Furcatopanorpa*

Furcatopanorpa is unique in Panorpidae in that the male adult lacks a notal organ on the posterior margin of the third tergum, and assumes an unusual O-shaped mouth-to-mouth nuptial feeding position during copulation (Zhong et al. 2015). The wings are much longer than the abdomen. The median axis of the female medigynium is bifurcated distally (Ma and Hua 2011). The male genitalia bear a pair of elongate hypovalves, which extend well beyond the apex of gonocoxites (Hua and Cai 2009; Zhong et al. 2015). In the male internal reproductive system, the epididymis is far apart from the testis, not appressed against the lateral base of the testis as in other genera (Zhang et al. 2016). These characters make *Furcatopanorpa* easily distinguished from the other genera of Panorpidae.

Furcatopanorpa was previously regarded as a sister group with all the other genera of Panorpidae based on a morphological phylogenetic analysis (Ma et al. 2012). A molecular phylogenetic analysis, however, indicates that *Furcatopanorpa* forms the sister group to *Panorpa* species from Northeastern Asia (Hu et al. 2015; Miao et al. 2019). Hu et al. (2015) suggested that *Furcatopanorpa* diverged from *Panorpa*, but here we confirm that *Furcatopanorpa* is the sister taxon to *Neopanorpa* based on phylogenetic analyses from mitogenomes. Although some features of the mitochondrial genome may generate misleading phylogenetic signals to cause problems such as long branch attraction, recent studies have found ways to avoid non-phylogenetic signal, such as using the site-heterogeneous mixture model, the inclusion of ribosomal RNA genes, and removal of fast-evolving sites (Song et al. 2016; Feuda et al. 2017; Liu et al. 2018). Based on the present analysis, the phylogenetic topologies of Panorpidae are generally very similar under standard models and the site-heterogeneous mixture model, indicating that the phylogenetic trees are considerably robust at the genus level.

Furcatopanorpa had unique cytogenetic features by large heterochromatic blocks occupying most of the chromosome length, suggesting that multiplied chromosome rearrangements might lead to considerable divergence between *Furcatopanorpa* and other genera of Panorpidae (Miao et al. 2019). *Furcatopanorpa* and most species of *Neopanorpa* have a similar number of chromosomes (n = 21) (Miao et al. 2019), also implying that *Furcatopanorpa* and *Neopanorpa* have a closer evolutionary relationship. In contrast, several species of *Panorpa*, such as *P. japonica*, *P. kunmingensis*, *P. liui*, and *P. macrostyla*, have different numbers of chromosomes (n = 23 or 24) (Miao et al. 2019), indicating a comparatively remote relationship.

Neopanorpa is regarded paraphyletic with *Leptopanorpa* based on a molecular (Miao et al. 2019) and a morphological phylogenetic analysis in Panorpidae (Wang and Hua 2020). Based on the present study, *Neopanorpa* forms a sister taxon to *Furcatopanorpa*. Nevertheless, since the genus *Leptopanorpa* is unfortunately not available in this study, and the two newly erected genera *Lulilan* and *Phine* are also not included in the analysis, the precise phylogenetic position of *Neopanorpa* awaits further research.

Panorpa Linnaeus, 1758 was considered paraphyletic with *Neopanorpa* according to a phylogenetic analysis from mitochondrial gene fragments (Misof et al. 2000). The paraphyly of *Panorpa* was confirmed with *Sinopanorpa*, *Dicerapanorpa*, and *Cerapanorpa* based on recent morphological and molecular phylogenetic studies (Ma et al. 2012; Hu et al. 2015; Miao et al. 2019). Our present phylogenetic analysis from mitogenomes further confirms that *Panorpa* is a paraphyletic group, which definitely needs a comprehensive taxonomic revision. The monophylies of *Cerapanorpa*, *Sinopanorpa*, and *Dicerapanorpa* are all confirmed, consistent with previous studies (Miao et al. 2019; Wang and Hua 2021).

Admittedly, mitogenomes are not available yet for the Indonesian genus *Leptopanorpa* MacLachlan, 1875 and recently erected genera *Megapanorpa* Wang & Hua, 2019, *Lulilan* Willmann, 2022 and *Phine* Willmann, 2022, and even some species groups of *Panorpa*, such as the *P. guttata* group, the Japanese *P. pryeri* group, and western Indian species. This study can only provide some new insights into the putative phylogenetic position of *Furcatopanorpa*.

4.3. Divergence time

Based on the present study, *Furcatopanorpa* is likely one of the earliest genera diversified in Panorpidae. The divergence time to the most recent common ancestor of *Neopanorpa* was approximately at 49.07 Ma, slightly earlier than the results of a previous study (ca. 42.1 Ma) (Miao et al. 2019).

The Panorpidae was supposed to originated from East Asia (Byers 1988; Miao et al. 2019), and migrated to North America via the Bering land bridge from early Paleocene to Pliocene (Sanmartín et al. 2001; Tiffney and Manchester 2001). Nevertheless, practically all the samples in this study were collected from China, only *P. debilis* was from North America. The migration route of Panorpidae can be better explained provided more specimens from Europe and North America are included in future studies.

5. Conclusions

In this paper, we used mitochondrial genomes to analyze the sequence architecture and to reconstruct the phylogeny of Panorpidae for the first time. *Furcatopanorpa* is the sister taxon to *Neopanorpa*, and is unsuitable to be assigned into the subfamily Panorpinae. We putatively conclude that *Furcatopanorpa* may deserve a subfamily status from the mitogenomic study.

6. Author Contributions

Data curation, YH and NL; Funding acquisition, YH, BZH and SHT; Investigation, YH and NL; Methodology, YH, NL, and JS; Project administration, YH, SHT and BZH; Software, YH, NL and JS; Supervision, LXX and SHT; Writing—original draft, YH and NL; Writing—review and editing, BZH, SHT, and LXX. All authors have read and agreed to the published version of the manuscript.

7. Competing interests

The authors declare that they have no competing interests.

8. Acknowledgments

We are grateful to Kai Gao, Lu Liu, Xin Tong, Ying Miao, and Xiao-Yan Wang for assistance in collecting specimens. This work was funded by the National Natural Science Foundation of China (Grant numbers 32100347, 31771474, and 31172125) and the China Postdoctoral Science Foundation (2020M683691XB).

9. References

Archibald SB, Bossert WH, Greenwood DR, Farrell BD (2010) Seasonality, the latitudinal gradient of diversity, and Eocene insects. Paleobiology 36: 374–398. https://doi.org/10.1666/09021.1

Archibald SB, Mathewes RW, Greenwood DR (2013) The Eocene Apex of panorpoid scorpionfly family diversity. Journal of Paleontology 87: 677–695. https://doi.org/10.1666/12-129

Beckenbach AT (2011) Mitochondrial genome sequences of representatives of three families of scorpionflies (Order Mecoptera) and evolution in a major duplication of coding sequence. Genome 54: 368–376. https://doi.org/10.1139/g11-006

Benson G (1999) Tandem repeats finder: a program to analyze DNA sequences. Nucleic Acids Research 27: 573–580. https://doi.org/10.1093/nar/27.2.573

Bergsten J (2005) A review of long-branch attraction. Cladistics 21(2): 163–193. https://doi.org/10.1111/j.1096-0031.2005.00059.x

Bernt M, Donath A, Jühling F, Externbrink F, Florentz C, Fritzsch G, Pütz J, Middendorf M, PF Stadler (2013) MITOS: improved de novo metazoan mitochondrial genome annotation. Molecular Phylogenetics and Evolution 69: 313–319. https://doi.org/10.1016/j.ympev.2012.08.023

Boore JL (1999) Animal mitochondrial genomes. Nucleic Acids Research 27: 1767–1780. https://doi.org/10.1093/nar/27.8.1767

Byers GW (1988) Geographic affinities of the North American Mecoptera. The Memoirs of the Entomological Society of Canada 120: 25–30. https://doi.org/10.4039/entm120144025-1

Cameron SL (2014) Insect mitochondrial genomics: implications for evolution and phylogeny. Annual Review of Entomology 59: 95–117. https://doi.org/10.1146/annurev-ento-011613-162007

Chen S, Zhou Y, Chen Y, Gu J (2018) fastp: an ultra-fast all-in-one FASTQ preprocessor. Bioinformatics 34: i884–i890. https://doi.org/10.1093/bioinformatics/bty560

Choudhary JS, Naaz N, Prabhakar CS, Rao MS, Das B (2015) The mitochondrial genome of the peach fruit fly, *Bactrocera zonata* (Saunders) (Diptera: Tephritidae): Complete DNA sequence, genome organization, and phylogenetic analysis with other tephritids using next generation DNA sequencing. Gene 569: 191–202. https://doi.org/10.1016/j.gene.2015.05.066

Cooper JK, Sykes G, King S, Cottrill K, Ivanova NV, Hanner R, Ikonomi P (2007) Species identification in cell culture: a two-pronged molecular approach. In Vitro Cellular & Developmental Biology-Animal 43: 344–351. https://doi.org/10.1007/s11626-007-9060-2

Demari-Silva B, Foster PG, de Oliveira TM, Bergo ES, Sanabani SS, Pessôa R, Sallum MAM (2015) Mitochondrial genomes and comparative analyses of *Culex camposi*, *Culex coronator*, *Culex usquatus* and *Culex usquatissimus* (Diptera: Culicidae), members of the coronator group. BMC Genomics 16: 831. https://doi.org/10.1186/s12864-015-1951-0

Dowton M, Castro L, Austin A (2002) Mitochondrial gene rearrangements as phylogenetic characters in the invertebrates: the examination of genome 'morphology'. Invertebrate Systematics 16: 345–356. https://doi.org/10.1071/IS02003

Drummond AJ, Suchard MA, Xie D, Rambaut A (2012) Bayesian phylogenetics with BEAUti and the BEAST 1.7. Molecular Biology and Evolution 29: 1969–1973. https://doi.org/10.1093/molbev/mss075

Hu GL, Yan G, Xu H, Hua BZ (2015) Molecular phylogeny of Panorpidae (Insecta: Mecoptera) based on mitochondrial and nuclear genes. Molecular Phylogenetics and Evolution 85: 22–31. https://doi.org/10.1016/j.ympev.2015.01.009

Hua BZ, Cai LJ (2009) A new species of the genus *Panorpa* (Mecoptera: Panorpidae) from China with notes on its biology. Journal of Natural History 43: 545–552. https://doi.org/10.1080/00222930802610519

Jia WZ, Yan HB, Guo AJ, Zhu XQ, Wang YC, Shi WG, Chen HT, Zhan F, Zhang SH, Fu BQ (2010) Complete mitochondrial genomes of *Taenia multiceps*, *T. hydatigena* and *T. pisiformis*: additional molecular markers for a tapeworm genus of human and animal health significance. BMC Genomics 11: 447. https://doi.org/10.1186/1471-2164-11-447

Kalyaanamoorthy S, Minh BQ, Wong TK, von Haeseler A, Jermiin LS (2017) ModelFinder: fast model selection for accurate phylogenetic estimates. Nature Methods 14: 587–589. https://doi.org/10.1038/nmeth.4285

Katoh K, Standley DM (2013) MAFFT multiple sequence alignment software version 7: improvements in performance and usability. Molecular Biology and Evolution 30: 772–780. https://doi.org/10.1093/molbev/mst010

Kumar S, Stecher G, Li M, Knyaz C, Tamura K (2018) MEGA X: molecular evolutionary genetics analysis across computing platforms. Molecular Biology and Evolution 35: 1547. https://doi.org/10.1093/molbev/msy096

Lanfear R, Frandsen PB, Wright AM, Senfeld T, Calcott B (2017) PartitionFinder 2: new methods for selecting partitioned models of evolution for molecular and morphological phylogenetic analyses. Molecular Biology and Evolution 34: 772–773. https://doi.org/10.1093/molbev/msw260

Lartillot N, Rodrigue N, Stubbs D, Richer J (2013) Phylobayes mpi: phylogenetic reconstruction with infinite mixtures of profiles in a parallel environment. Systematic Biology 62(4): 611-615. https://doi.org/10.1093/sysbio/syt022

Li K, Liang AP (2018) Hemiptera mitochondrial control region: new sights into the structural organization, phylogenetic utility, and roles of tandem repetitions of the noncoding segment. International Journal of Molecular Sciences 19: 1292. https://doi.org/10.3390/ijms19051292

Li N, Hu GL, Hua BZ (2019) Complete mitochondrial genomes of *Bittacus strigosus* and *Panorpa debilis* and genomic comparisons of Mecoptera. International Journal of Biological Macromolecules 140: 672–681. https://doi.org/10.1016/j.ijbiomac.2019.08.152

Lobry J (1995) Properties of a general model of DNA evolution under no-strand-bias conditions. Journal of Molecular Evolution 40: 326–330. https://doi.org/10.1007/BF00163237

Lohse M, Drechsel O, Kahlau S, Bock R (2013) OrganellarGenomeDRAW—a suite of tools for generating physical maps of plastid and mitochondrial genomes and visualizing expression data sets. Nucleic Acids Research 41: W575–W581. https://doi.org/10.1093/nar/gkt289

Ma LY, Liu FF, Chiba H, Yuan XQ (2020) The mitochondrial genomes of three skippers: Insights into the evolution of the family Hesperiidae (Lepidoptera). Genomics 112: 432–441. https://doi.org/10.1016/j.ygeno.2019.03.006

Ma N, Hua BZ (2011) *Furcatopanorpa*, a new genus of Panorpidae (Mecoptera) from China. Journal of Natural History 45: 2247–2257. https://doi.org/10.1080/00222933.2011.595517

Ma N, Zhong W, Gao QH, Hua BZ (2012) Female genital plate diversity and phylogenetic analyses of East Asian Panorpidae (Mecoptera). Systematics and Biodiversity 10: 159–178. https://doi.org/10.1080/14772000.2012.683459

Meng GL, Li YY, Yang CT, Liu SL (2019) MitoZ: a toolkit for animal mitochondrial genome assembly, annotation and visualization. Nucleic Acids Research 47: e63–e63. https://doi.org/10.1093/nar/gkz173

Miao Y, Wang JS, Hua BZ (2019) Molecular phylogeny of the scorpionflies Panorpidae (Insecta: Mecoptera) and chromosomal evolution. Cladistics 35: 385–400. https://doi.org/10.1111/cla.12357

Misof B, Erpenbeck D, Sauer K (2000) Mitochondrial gene fragments suggest paraphyly of the genus *Panorpa* (Mecoptera, Panorpidae). Molecular Phylogenetics and Evolution 17: 76–84. https://doi.org/10.1006/mpev.2000.0817

Monforte A, Barrio E, Latorre A (1993) Characterization of the length polymorphism in the A+ T-rich region of the *Drosophila obscura* group species. Journal of Molecular Evolution 36: 214–223. https://doi.org/10.1007/BF00160476

Nguyen LT, Schmidt HA, von Haeseler A, Minh BQ (2015) IQ-TREE: a fast and effective stochastic algorithm for estimating maximum-likelihood phylogenies. Molecular Biology and Evolution 32: 268–274. https://doi.org/10.1093/molbev/msu300

Nie RE, Andújar C, Gómez-Rodríguez C, Bai M, Xue HJ, Tang M, Yang CT, Tang P, Yang XK, Vogler AP (2020) The phylogeny of leaf beetles (Chrysomelidae) inferred from mitochondrial genomes. Systematic Entomology 45(1): 188–204. https://doi.org/10.1111/syen.12387

Parham JF, Donoghue PC, Bell CJ, Calway TD, Head JJ, Holroyd PA, Inoue JG, Irmis RB, Joyce WG, Ksepka DT (2012) Best practices for justifying fossil calibrations. Systematic Biology 61: 346–359. https://doi.org/10.1093/sysbio/syr107

Rambaut A, Drummond AJ, Xie D, Baele G, Suchard MA (2018) Posterior summarization in Bayesian phylogenetics using Tracer 1.7. Systematic Biology 67: 901–904. https://doi.org/10.1093/sysbio/syy032

Ronquist F, Teslenko M, van Der Mark P, Ayres DL, Darling A, Höhna S, Larget B, Liu L, Suchard MA, Huelsenbeck JP (2012) MrBayes 3.2: efficient Bayesian phylogenetic inference and model choice across a large model space. Systematic Biology 61: 539–542. https://doi.org/10.1093/sysbio/sys029

Rozas J, Sánchez-DelBarrio JC, Messeguer X, Rozas R (2003) DnaSP, DNA polymorphism analyses by the coalescent and other methods. Bioinformatics 19: 2496–2497. https://doi.org/10.1093/bioinformatics/btg359

Sanmartín I, Enghoff H, Ronquist F (2001) Patterns of animal dispersal, vicariance and diversification in the Holarctic. Biological Journal of the Linnean Society 73: 345–390. https://doi.org/10.1111/j.1095-8312.2001.tb01368.x

Song F, Li H, Jiang P, Zhou XG, Liu JP, Sun CH, Vogler AP, Cai WZ (2016) Capturing the phylogeny of Holometabola with mitochondrial genome data and Bayesian site-heterogeneous mixture models. Genome Biology and Evolution 8: 1411–1426. https://doi.org/10.1093/gbe/evw086

Talavera G, Castresana J (2007) Improvement of phylogenies after removing divergent and ambiguously aligned blocks from protein sequence alignments. Systematic Biology 56: 564–577. https://doi.org/10.1080/10635150701472164

Tiffney BH, Manchester SR (2001) The use of geological and paleontological evidence in evaluating plant phylogeographic hypotheses in the Northern Hemisphere Tertiary. International Journal of Plant Sciences 162: S3–S17. https://doi.org/10.1086/323880

Wang JS, Hua BZ (2018) A color atlas of the Chinese Mecoptera. Henan Science and Technology Press, Zhengzhou, 315–420. https://doi.org/10.1007/978-981-16-9558-2

Wang JS, Hua BZ (2020) Taxonomic revision and phylogenetic analysis of the enigmatic scorpionfly genus *Leptopanorpa* MacLachlan (Mecoptera: Panorpidae). Journal of Zoological Systematics and Evolutionary Research 58: 900–928. https://doi.org/10.1111/jzs.12363

Wang, JS, Hua BZ (2021) Morphological phylogeny of Panorpidae (Mecoptera: Panorpoidea). Systematic Entomology 46: 526–557. https://doi.org/10.1111/syen.12474

Wang Y, Huang XL, Qiao GX (2013) Comparative analysis of mitochondrial genomes of five aphid species (Hemiptera: Aphididae) and phylogenetic implications. PLoS One 8: e77511. https://doi.org/10.1371/journal.pone.0077511

Wang Y, Cao JJ, Li N, Ma GY, Li WH (2019) The first mitochondrial genome from Scopuridae (Insecta: Plecoptera) reveals structural features and phylogenetic implications. International Journal of Biological Macromolecules 122: 893–902. https://doi.org/10.1016/j.ijbiomac.2018.11.019

Wei SJ, Shi M, Chen XX, Sharkey MJ, van Achterberg C, Ye GY, He JH (2010) New views on strand asymmetry in insect mitochondrial genomes. PLoS One 5: e12708. https://doi.org/10.1371/journal.pone.0012708

Willmann R (2022) Neue Skorpionsfliegen (Mecoptera, Panorpidae) aus Nepal. Contributions to Entomology 72(2): 309–320. https://doi.org/10.3897/contrib.entomol.72.e97277

Zhang BB, Lyu QH, Hua BZ (2016) Male reproductive system and sperm ultrastructure of *Furcatopanorpa longihypovalva* (Hua and Cai, 2009)(Mecoptera: Panorpidae) and its phylogenetic implication. Zoologischer Anzeiger 264: 41–46. https://doi.org/10.1016/j.jcz.2016.07.004

Zhang D, Zou H, Wu SG, Li M, Jakovlić I, Zhang J, Chen R, Li WX, Wang GT (2018) Three new Diplozoidae mitogenomes expose unusual compositional biases within the Monogenea class: implications for phylogenetic studies. BMC Evolutionary Biology 18: 133. https://doi.org/10.1186/s12862-018-1249-3

Zhang D, Gao FL, Jakovlić I, Zou H, Zhang J, Li WX, Wang GT (2020) PhyloSuite: an integrated and scalable desktop platform for streamlined molecular sequence data management and evolutionary phylogenetics studies. Molecular Ecology Resources 20: 348–355. https://doi.org/10.1111/1755-0998.13096

Zhang DX, Hewitt GM (1997) Insect mitochondrial control region: a review of its structure, evolution and usefulness in evolutionary studies. Biochemical Systematics and Ecology 25: 99–120. https://doi.org/10.1016/S0305-1978(96)00042-7

Zhong W, Qi ZY, Hua BZ (2015) Atypical mating in a scorpionfly without a notal organ. Contributions to Zoology 84: 305–315. https://doi.org/10.1163/18759866-08404003

Supplementary Material 1

Tables S1–S3

Authors: Hua Y, Li N, Su J, Hua BZ, Tao SH, Xing LX (2024)
Data type: .pdf
Explanation notes: Table S1. Base composition and strand bias of Panorpidae. — **Table S2.** Best partitioning scheme and models based on different datasets for Bayesian inference (BI) analysis selected by PartitionFinder. — **Table S3.** Best partitioning scheme and models based on different datasets for Maximum likelihood (ML) analysis selected by ModelFinder.

Link: https://doi.org/10.3897/asp.82.e105560.suppl1

Supplementary Material 2

Figures S1–S11

Authors: Hua Y, Li N, Su J, Hua BZ, Tao SH, Xing LX (2024)

Data type: .pdf

Explanation notes: Figures S1, S2. Relative synonymous codon usage (RSCU) of Panorpidae mitogenomes. — **Figure S3.** Sliding window analysis of 13 PCGs and two rRNAs. The blue curve shows the value of nucleotide diversity (π) above the arrows. — **Figure S4.** Evolutionary rates and selection pressures among 48 mitogenomes of Panorpidae. Genetic distance and ratio of non-synonymous (Ka) to synonymous (Ks) substitution rates of each protein-coding gene. — **Figure S5.** Phylogenetic tree generated by Bayesian inference and maximum likelihood based on the dataset of PCG. Numerals at nodes are Bayesian posterior probabilities (PP) and bootstrap support values (BS). — **Figure S6.** Phylogenetic tree generated by Bayesian inference and maximum likelihood based on the dataset of PCG + RT. Numerals at nodes are Bayesian posterior probabilities (PP) and bootstrap support values (BS). — **Figure S7.** Phylogenetic tree generated by Bayesian inference and maximum likelihood based on the dataset of PCG12 + R. Numerals at nodes are Bayesian posterior probabilities (PP) and bootstrap support values (BS). — **Figure S8.** Bayesian inference tree generated by Phylobayes with CAT-GTR model based on the dataset of PCG. Numerals at nodes are Bayesian posterior probabilities (PP). — **Figure S9.** Bayesian inference tree generated by Phylobayes with CAT-GTR model based on the dataset of PCG + R. Numerals at nodes are Bayesian posterior probabilities (PP). — **Figure S10.** Bayesian inference tree generated by Phylobayes with CAT-GTR model based on the dataset of PCG + RT. Numerals at nodes are Bayesian posterior probabilities (PP). — **Figure S11.** Bayesian inference tree generated by Phylobayes with CAT-GTR model based on the dataset of PCG12 + R. Numerals at nodes are Bayesian posterior probabilities (PP).

Link: https://doi.org/10.3897/asp.82.e105560.suppl2